Journal of Catalysis **194,** 401–409 (2000)
doi:10.1006/jcat.2000.2955, available online at http://www.idealibrary.com on IDEAL®

Infrared Study of CO Adsorbed on a Co/Re/γAl$_2$O$_3$-Based Fischer–Tropsch Catalyst

L. E. S. Rygh and C. J. Nielsen

Department of Chemistry, University of Oslo, P.O.Box 1033, N-0315 Oslo, Norway

Received February 28, 2000; revised June 5, 2000; accepted June 7, 2000

The adsorption of CO(g) on a Co/Re/γ-Al$_2$O$_3$ catalyst has been studied by diffuse reflectance infrared spectroscopy. The effects of pressure and temperature as well as addition of O$_2$(g) and H$_2$(g) have been investigated. The presence of Re as a promoter is shown to increase the degree of cobalt reduction, increase the amount of bridged species, and decrease the reduction temperature without any sign of electronic interaction between the two metals. Oxidation or hydrogenation reveals bands arising from rhenium carbonyl species, showing that the Re is located at the catalyst surface. It is proposed that Re either by direct blocking or by sterical hindrance inhibits the transportation of formate onto the active Co sites, and thereby hinders one of two possible reaction paths in the Fischer–Tropsch synthesis. When the catalyst is exposed to low pressures of CO for longer periods new band structures appear, suggesting that exposure to CO may lead to a reconstruction of the Co surface. This process involves creation/destruction of various adsorption sites and leads to a decrease in the long-range dipole–dipole interaction. Consequently, new absorptions are revealed in the spectrum.

Key Words: **Fischer–Tropsch; CO hydrogenation; carbon monoxide; cobalt; rhenium; promoter; promoting effects; bimetallic catalyst; infrared; DRIFTS.**

I. INTRODUCTION

In this work, we report our studies of the Fischer–Tropsch reaction on a 12% Co/Re/γ-Al$_2$O$_3$ catalyst. The assignment of the infrared bands is based on our previous study of a 12% Co/γ-Al$_2$O$_3$ catalyst (1). This study included a theoretical model which enables the calculation of absorptions arising from CO being adsorbed on various sites on the Co surface (1). Infrared studies of other Co/Al$_2$O$_3$ catalysts (2–11), cobalt films or foils (12–21), cobalt single crystals (22–25), cobalt oxides (26), cobalt carbonyls (27–30), and cobalt alumina spinel (31) supply additional information. So do other studies of Co/Re/Al$_2$O$_3$ catalysts (32–35).

II. EXPERIMENTAL

DRIFTS (diffuse reflectance infrared fourier transform spectroscopy) spectra were recorded with a Perkin Elmer model 2000 FTIR instrument using a spectral resolution of 8 cm^{-1}. The DRIFT unit including a vacuum chamber was obtained from Harrick Sci. Corp. For information about DRIFTS for heterogeneous catalyst studies, see Refs. (36, 37). All spectra presented here are transformed into Kubelka–Munk units.

The reactants were introduced via a gas-handling manifold including a glass mixing chamber. An absolute pressure transducer from Balzers was used to measure the pressure. The purities of the gases used in the experiments were 99.997% (CO), 99.9997% (H$_2$), 99.998% (O$_2$), and 99.9995% (N$_2$). Furthermore, the gases were cleaned prior to use by passing them through the following gas purifiers from Supelco: an OMI-1 indicating purifier (H$_2$ and N$_2$), a Supelpure O-trap (CO), and a drying tube, molecular sieve 5A (CO, O$_2$). Contamination from oxygen should be reduced to less than 0.5 ppm by this procedure.

The 12% Co/1% Re/γ-Al$_2$O$_3$ catalyst was made by impregnating γ-Al$_2$O$_3$ (Akzo, Alumina 000-1 1/2 E) with an aqueous solution of Co(NO$_3$)$_2 \cdot 6$H$_2$O + HReO$_4$ (coprecipitation), using the incipient wetness technique. Subsequently, the samples were dried at 100°C and calcinated at 300°C.

The catalyst was reduced *in situ* for 16–20 h under atmospheric pressure by a stream of H$_2$ at 400°C. Subsequently, the system was cooled to the desired temperature before evacuation and following introduction of CO(g). The CO pressure was typically 1–150 mbar, and the CO adsorption was studied as a function of temperature (30–400°C) and time, before and after the catalyst surface was exposed to additional H$_2$ or O$_2$. Temperature changes were performed at a rate of 1–2 deg min^{-1}. The total exposure time was normally a few hours, until no further spectral developments were observed.

III. THEORETICAL MODEL FOR SPECTRAL ASSIGNMENTS AT LOW SURFACE COVERAGE

An empirical relationship between the number of valence electrons and the carbonyl stretching frequency has been found for carbonyl complexes of transition

0021-9517/00 $35.00

metals (38). In this relation, the force constants for metal carbonyl complexes are expressed in terms of the number of valence electrons of the metal atom, and the ionic charge of the complex and of the various ligands. Essentially, the model is a parametrization of the number of electrons available for bonding. The $Co(CO)_x$ ($x = 1$–4) species found on Co surfaces are very "complex-like," as they are rather loosely attached to the neighboring cobalt atoms and are able to migrate along the metal surface. Consequently, the only modification we have introduced to the model presented by Timney (38) is to replace the combined contribution from ionic charge and ligand effects by a calculated number of valence electrons for the individual cobalt atoms.

The number of available electrons on various surfaces and on edges and corners was obtained by ASED-MO (extended Hückel) calculations (39, 40). To perform these calculations we employed a quantum chemistry program ICONC&INPUTC developed by Calzaferri and Brändle (41). However, it is necessary to have data for the atomic valence orbital ionization potentials and the Slater orbital exponents. Using this program, we have not experienced any problems with metal cluster models consisting of as much as 160–200 atoms depending on the symmetry of the actual cluster. Primarily, we aimed to find the number of valence electrons typical of Co atoms situated well within the various surface planes, that is, as far away from the edges/corners as possible. This number is best approximated by the theoretical values calculated for the Co atoms situated in the middle of the model surfaces. The models are such that 2.4 to 4 atoms in all directions surround various central surface atoms. The number of valence electrons for Co atoms situated at edges/corners was estimated in a similar manner. For more details, see Ref. (1).

IV. RESULTS

A typical spectrum of the 12% Co/1% Re/γ-Al_2O_3 catalyst is presented in Fig. 1a. The effects of evacuation, temperature, exposure time, oxidation and hydrogenation are shown in the Figs. 2–7, respectively. In general, we found that the band structures that developed after exposure to CO(g) were nearly identical, both in appearance and in behavior, to those characteristic of the monometallic catalyst (Fig. 1b). Nevertheless, the bimetallic catalyst differs from the monometallic in certain points:

- The bimetallic catalyst apparently reaches the same degree of reduction at 400 as at 500°C, while the monometallic is much better reduced at 500°C (1) (Figs. 1b, 1c).
- The monometallic catalyst is very sensitive toward deviations from the ideal reduction conditions at 400°C, for example due to instabilities in the hydrogen flow. Poor reduction gives rise to intensity maxima that are of lower intensity and higher wavenumbers, and the low-wavenumber tail does not reveal any distinct intensity maxima even at low pressures of CO. In contrast, the bimetallic catalyst is easily reduced, and there are only small variances in the recorded spectra.
- The bimetallic catalyst invariantly gives rise to absorptions of substantially higher intensities than the monometallic catalyst. Due to the more intense absorptions, the spectra of the bimetallic catalyst are less noisy at low pressures of CO(g).
- The absorptions at 1880–1900 and 1820–10 cm^{-1}, assigned to bridged species, are both more frequently observed and show maxima that are more distinct[1] (Fig 1).

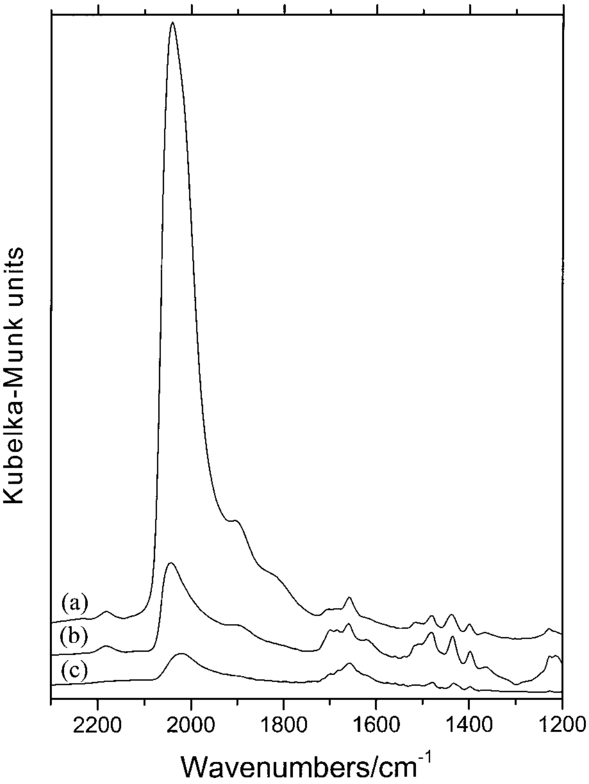

FIG. 1. FTIR spectrum of various catalyst samples recorded after 5 min of exposure to 1 mbar CO(g) at room temperature: (a) 12% Co/1% Re/γ-Al_2O_3 reduced at 400°C, (b) 12% Co/γ-Al_2O_3 reduced at 500°C, and (c) 12% Co/γ-Al_2O_3 reduced at 400°C.

Upon evacuation, the absorptions at high wavenumbers were the first to disappear, leaving a band at 1980 cm^{-1} after 15 min of evacuation (Fig. 2). Further, the band at 1900 cm^{-1} was hardly visible at CO pressures below 0.01 mbar, while the less intense band at 1810 cm^{-1} only disappeared after 15 min of evacuation.

---

[1] A band maximum at 1920–1900 cm^{-1} appears with a less defined peak between 1820 and 1805 cm^{-1} immediately after introduction of CO(g) at room temperature. These band maxima have been observed for P_{CO} as high as 30 mbar.

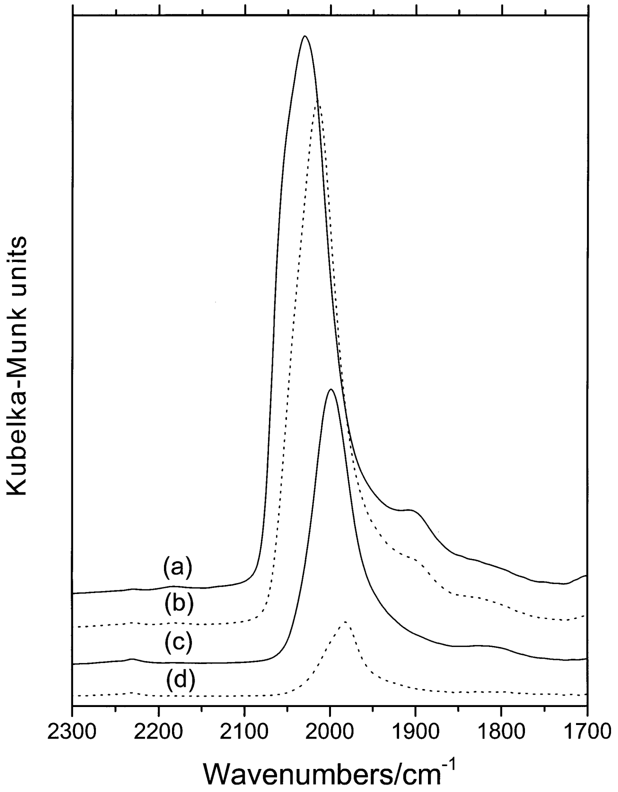

FIG. 2. FTIR spectra of CO on 12% Co/1% Re/γ-Al_2O_3 during evacuation at room temperature: (a) $P_{CO} = 1.2$ mbar, (b) $P_{CO} = 0.1$ mbar, (c) $P_{CO} < 0.01$ mbar, and (d) $P_{CO} \approx 1 \times 10^{-3}$ mbar (after 15 min of evacuation).

How the temperature influences the spectra is illustrated in Fig. 3. At room temperature, the spectrum showed an intensity maximum at 2060 cm^{-1}, with a shoulder appearing at 2030 cm^{-1} (Fig. 3a). When the temperature was raised to about 150–200°C, the intensity maximum increased (Figs. 3a–3e). Subsequently, the high-temperature intensity maximum decreased as a function of time. Further increases in the temperature made the intensity fall even more rapidly (Figs. 3e–3g). Also, the wavenumber of the intensity maximum was temperature dependent. When the temperature was raised from room temperature to 100°C, the maximum red-shifted 25 cm^{-1}, from 2060 to 2035 cm^{-1} (Figs. 3a, 3b). Ten minutes later the maximum had returned to 2060 cm^{-1}, simultaneously as a broad band began to grow around 1900 cm^{-1}, (Fig. 3c). From room temperature to 150°C, the intensity maximum experienced a slight blue shift and the absorptions in the high-wavenumber region became more pronounced. Simultaneously, the 1920 cm^{-1} band became more distinct (Figs. 3a–3d). From 150 to 250°C, we observed a red shift, which increased with annealing time (Figs. 3d–3h). After prolonged exposure to CO(g) at 250°C, all bands vanished except those that were due to the rhenium carbonyl species (Fig. 3i) (42). At room temperature and as a function of time, the intensity maximum

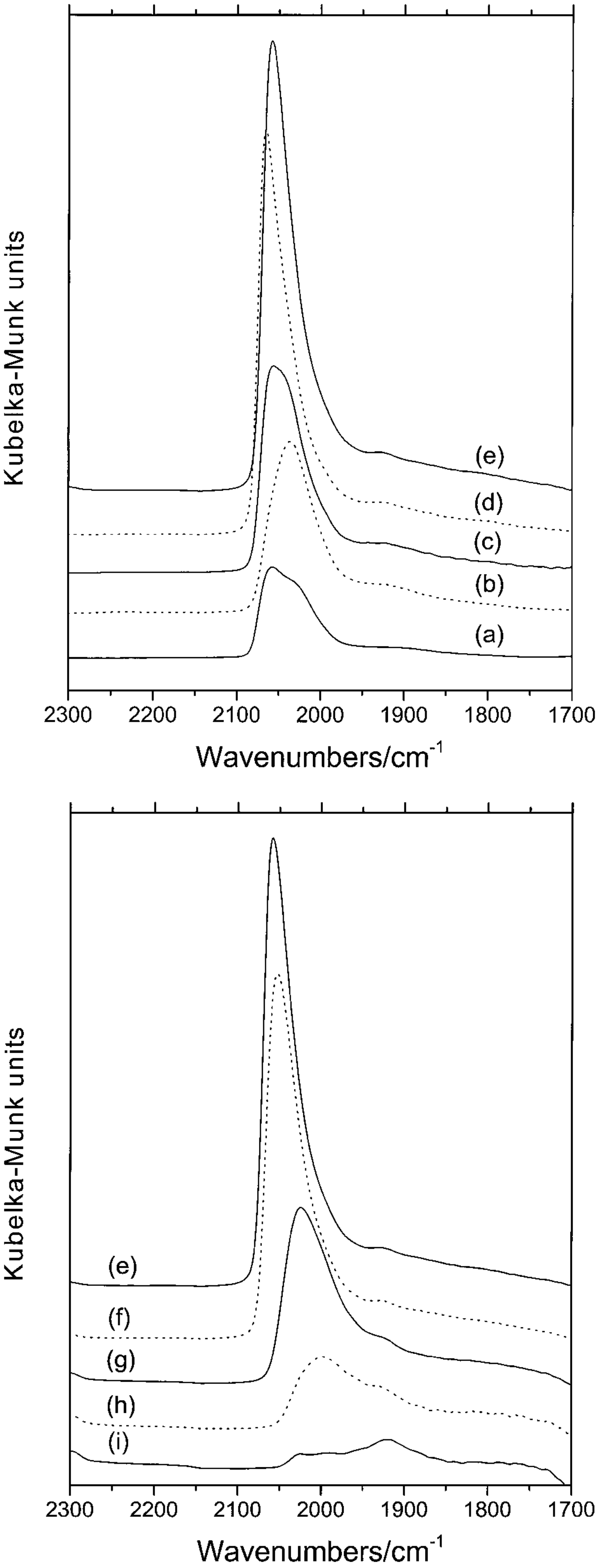

FIG. 3. FTIR spectra of CO on 12% Co/1% Re/γ-Al_2O_3 as a function of temperature, $P_{CO} = 25$ mbar: (a) after 1 h at room temperature, (b) after 10 min at 100°C, (c) after 1 h at 100°C, (d) after 10 min at 150°C, (e) after 20 min at 200°C, (f) after 55 min at 200°C, (g) after 5 min at 250°C, (h) after 1 h, 45 min at 250°C, and (i) after 18 h at 250°C.

increased and shifted to higher wavenumbers. At 200°C, the same development was observed at the outset, but at a certain point there was a fall in the intensity followed by a red shift (Fig. 4). Simultaneously, a low-wavenumber “tail” ranging from 1970 to 1850 cm^{-1} remained relatively constant. Nevertheless, after 3 h of CO exposure at 200°C, the intensity maximum had decreased to 1990 cm^{-1} and a new maximum became apparent at 1940 cm^{-1} (Fig. 4e). After prolonged exposure time, the spectrum would normally appear as in Fig. 3i.

The response to the introduction of O_2(g) or H_2(g), subsequent to the CO adsorption, is presented in Figs. 5 and 6. In the corresponding case of the monometallic catalyst, hydrogenation or oxidation could make all CO absorptions disappear from the spectrum. In contrast, we here observed new, very resistant bands at 2035, 1925, and 1895(sh) cm^{-1}. During the hydrogenation process, new distinct absorption maxima were also revealed between 1980 and 1925 cm^{-1} (Fig. 7).

At very low CO(g) pressures and 200°C, we observed various intensity maxima that were concealed by other more intense absorptions at higher pressures (Fig. 8). Our observations may be classified into two categories:

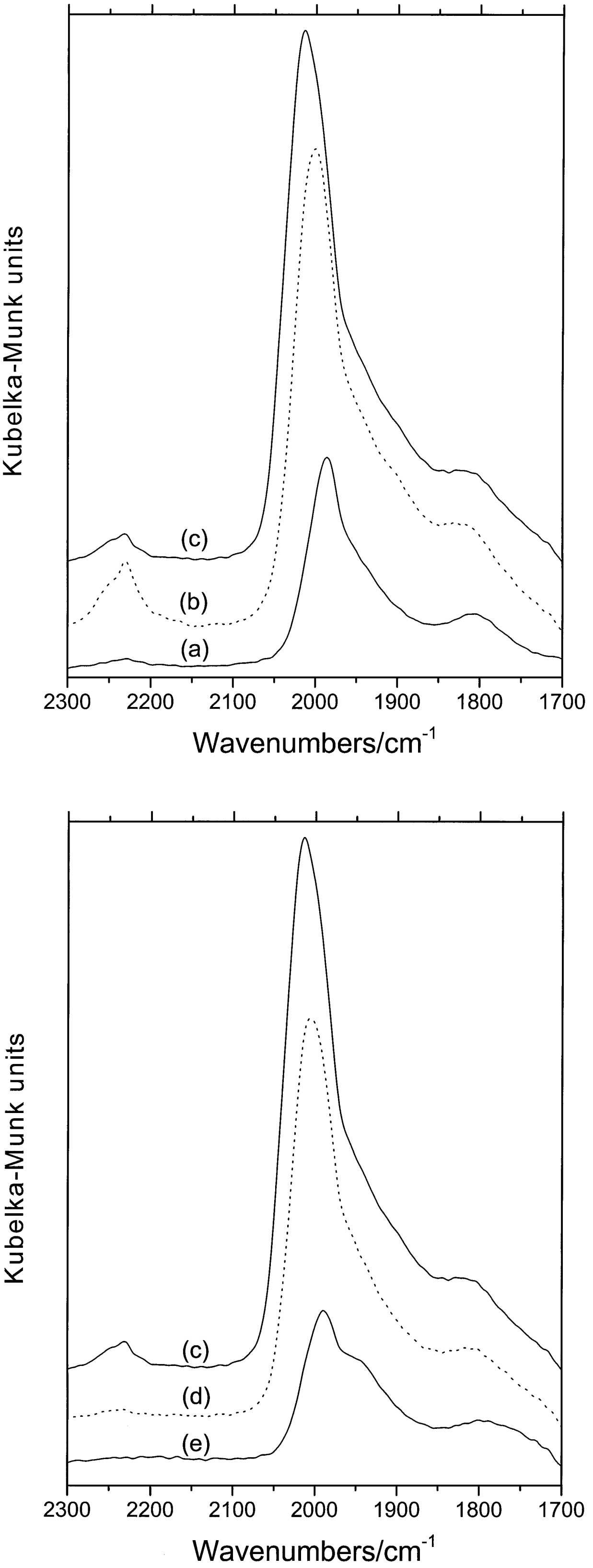

FIG. 4. FTIR spectra of CO on 12% Co/1% Re/γ-Al_2O_3 after exposure to CO(g) at 200°C: (a) $P_{CO} = 0.3$ mbar, (b) $P_{CO} = 1$ mbar, (c) after 25 min with $P_{CO} = 1$ mbar, (d) after 1 h, and (e) after 3 h 20 min.

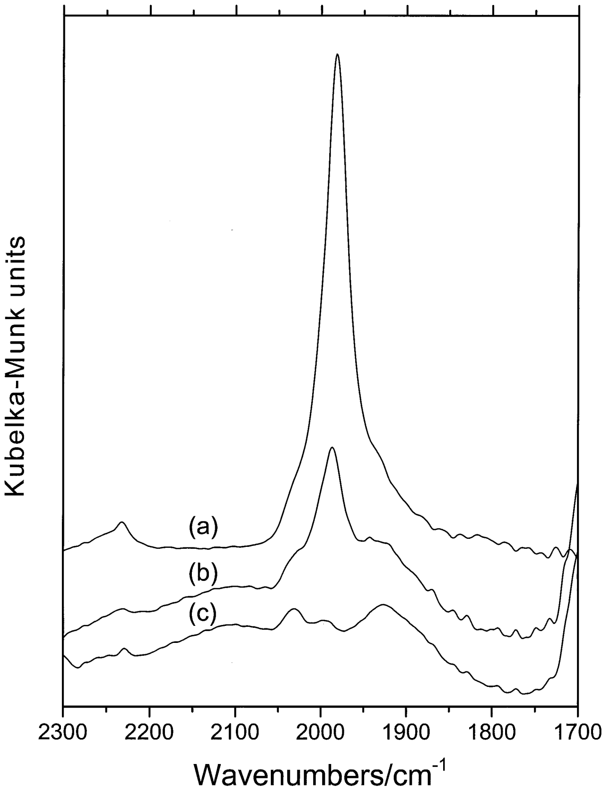

FIG. 5. FTIR spectra of CO on 12% Co/1% Re/γ-Al_2O_3 before and after oxidation at room temperature: (a) after 10 min of evacuation, (b) after 3.5 h with $P_{O_2} = 0.01$ mbar, and (c) after an additional 0.5 h with $P_{O_2} = 0.05$ mbar.

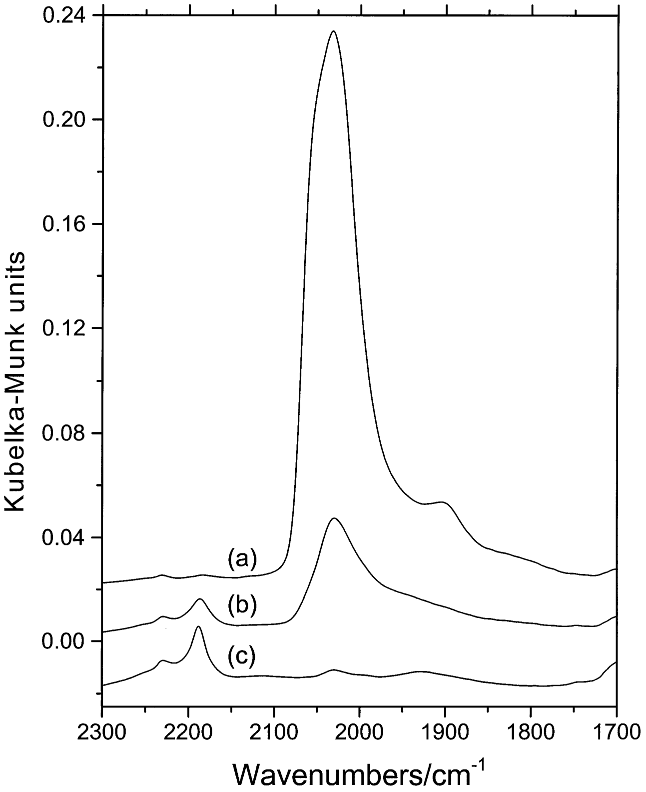

FIG. 6. FTIR spectra of CO on 12% Co/1% Re/γ-Al_2O_3 before and after hydrogenation at 200°C: (a) after 15 min with $P_{CO} = 1$ mbar, (b) after 8 min with Fischer–Tropsch activity ($P_{CO} = P_{H_2} = 1$ mbar), and (c) after 3 h.

(i) Only a single absorption band was observed at 1920–29 cm^{-1} (Fig. 8a).

(ii) Multiple bands with intensity maxima around the wavenumbers 1970–95, 1938–50, 1897–1900, 1806–20, and 1791–1800 cm^{-1} were observed in various combinations, as illustrated in Figs. 4a and 8b.

All the bands listed above are low in intensity, and there are some variations in the observed wavenumbers. The 1920 cm^{-1} band in the first category was observed at CO pressures $\ll$1 mbar, and the intensity maximum increased continuously toward 1990 cm^{-1} when the pressure was increased. Concerning the second category, the pressure of CO was here slightly higher (although still <1 mbar). The two bands in the region 1790–1820 cm^{-1} were not observed in the same spectra, while the 1990 and the 1950 cm^{-1} bands sometimes appeared simultaneously.

On one occasion, prolonged Fischer–Tropsch activity[2] was followed by evacuation, cooling to room temperature, and reintroduction of 150 mbar CO(g). After the system had been left for 2 days, new spectral features appeared. We observed absorption maxima at 2057, 2033, 1990(sh), 1937, 1937–45, 1893, and 1867 cm^{-1} (Fig. 9a). The same catalyst sample was subsequently reduced overnight at 500°C. Immediately after reintroduction of CO(g) at room temperature there was no sign of these band structures. However, the maxima became successively more distinct with exposure time. The band intensities increased steadily during several hours until they reached the same intensity as before the reduction procedure (Fig. 9b).

We also studied the reproducibility of the CO absorption bands at various temperatures. At room temperature, we found the CO adsorption to be nearly reversible. Exposure to CO(g) or syngas at 200°C followed by evacuation and subsequent reintroduction of CO led to absorption bands lower in both intensity and wavenumbers compared to the original bands. It was also impossible to re-establish the initial spectrum when the temperature was raised from 200 to 250°C, and shortly after lowered back to 200°C.

Results from our ASED-MO calculations and the calculated wavenumbers for $Co(CO)_x$ ($x = 1$–3) adsorbed on various surface sites (1) are presented in Table 1. We observe that the first CO molecules that adsorb on the Co(0001) surface are expected to give rise to absorptions around 1980 cm^{-1}. CO molecules adsorbed on coordinately

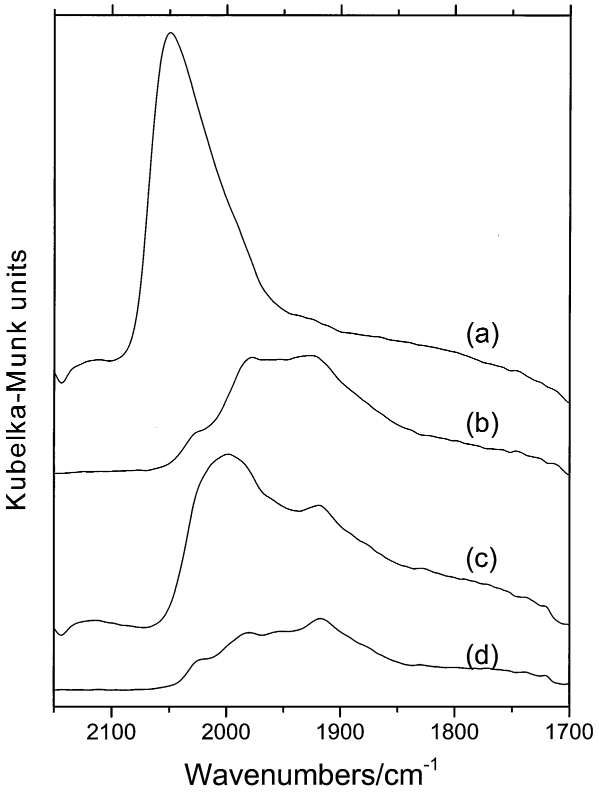

FIG. 7. FTIR spectra of CO on 12% Co/1% Re/γ-Al_2O_3 during hydrogenation at 250°C ($P_{CO} = 150$ mbar, $P_{H_2} = 300$ mbar). CO was preadsorbed for 20 min before introduction of H_2: (a) immediately before introduction of H_2, (b) after 35 min of exposure to H_2, (c) after 18 h, and (d) after 18 h and subsequent evacuation to $P_{tot} = 5$ mbar.

---

[2] 3 h at 200°C, followed by 18 h at 250°C; $P_{CO} = 150$ mbar, $P_{H_2} =$ 300 mbar.

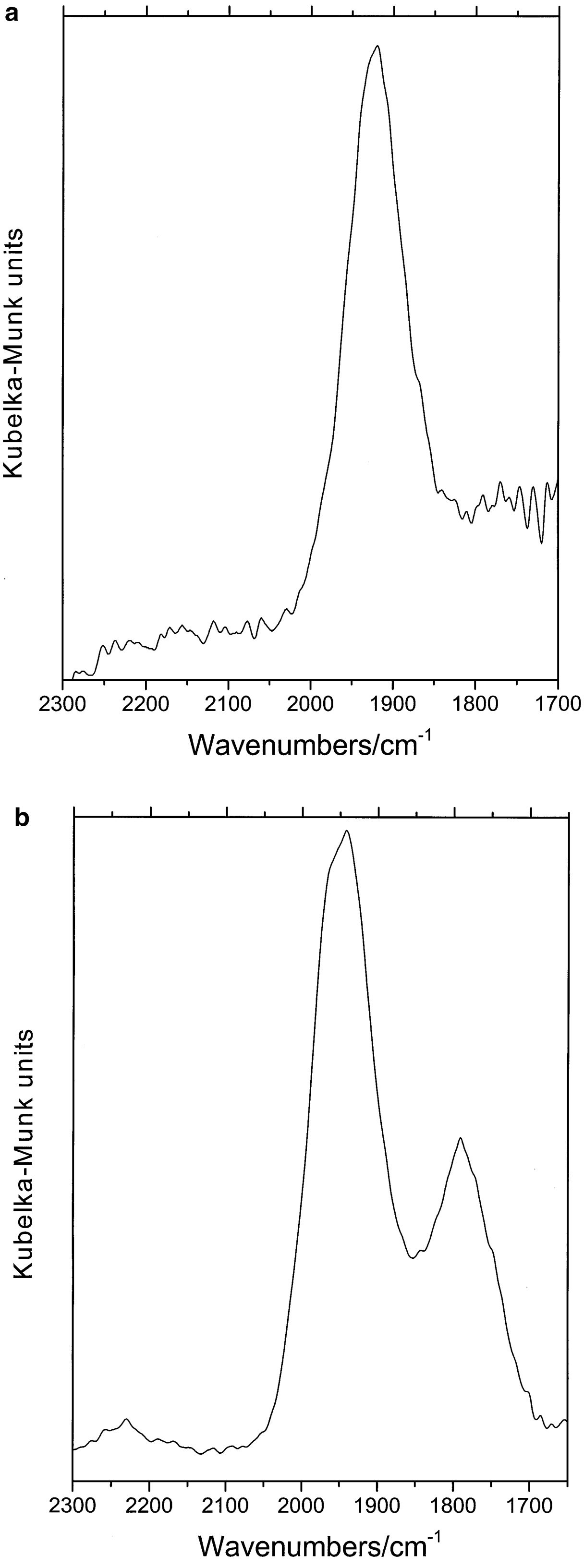

FIG. 8. FTIR spectra of CO on 12% Co/1% Re/γ-Al_2O_3 recorded immediately after introduction of small amounts of CO(g) (less than 1 mbar) at 200°C. See also Fig. 3a.

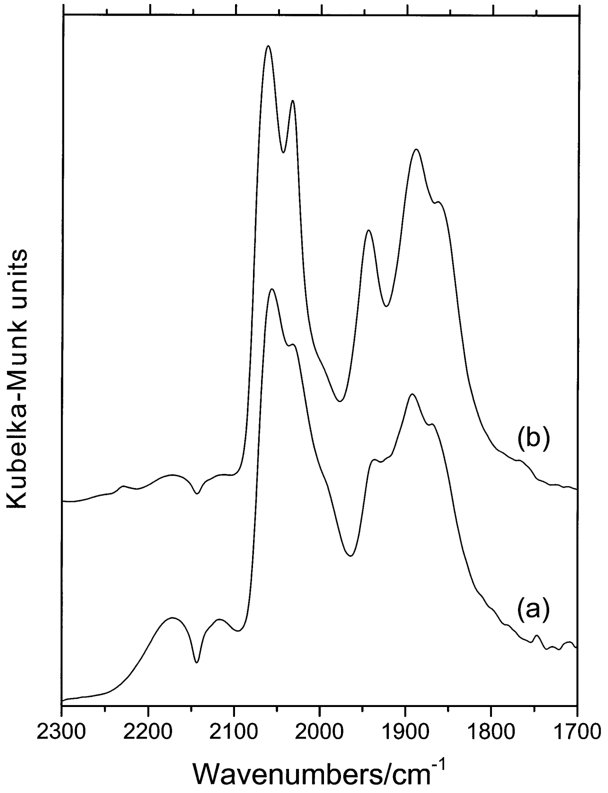

FIG. 9. FTIR spectra of CO on 12% Co/1% Re/γ-Al_2O_3 after prolonged exposure to CO(g) at room temperature: (a) 2 days with $P_{CO} =$ 150 mbar at room temperature (prehistory here includes hydrogenation at 250°C for 18 h), and (b) after subsequent oxidation at room temperature, reduction at 500°C, and new exposure to $P_{CO} = 150$ mbar for 22 h at room temperature.

unsaturated sites may contribute to absorptions as low as 1835 cm^{-1}. Concerning the subcarbonyls, the symmetric ν_s modes are expected to be more intense than the antisymmetric ν_a and the ν_e modes due to “the metal surface selection rule” (43, 44).

V. DISCUSSION

The spectra of CO adsorbed on the 12% Co/1% Re/γ-Al_2O_3 catalyst show that the presence of Re induces a (significant) general increase in the absorbances (Fig. 1). Simultaneously, the absorptions at 1880–1900 and 1820 cm^{-1}, assigned to bridged species, both are more frequently observed and show maxima that are more distinct than for the monometallic catalyst. These observations indicate that Re leads to a better-reduced Co surface and are well in accordance with other data (32). Small amounts of Re has been shown to increase the degree of reduction of the catalyst from ~50% to ~80%, triple the amount of CO adsorbed on Co, and approximately double the CO hydrogenation rate. Essentially, the addition of Re increases the concentration of active sites, while the average site activity is shown

TABLE 1

Number of Valence Electrons Characteristic of Different Co Atoms Situated at Various Planes, Edges, or Corners Estimated by ASED-MO Calculations, as Well as Vibrational Wavenumbers Calculated for Low Coverages of Mono- and Polycarbonyl Species on Various Planes, Edges, and Corners

Surface	No. of atoms	Calcd no. of valence electrons				$Co_m(CO)$	$Co_m(CO)_2$		$Co_m(CO)_3$	
		s	*p*	*d*	Total	ν_{CO}	ν_s	ν_a	ν_s	ν_d
Co(0001)	126	0.67	0.20	7.94	8.81	1978	2017	1977	2052	1997
Co(10-10)*	160	0.67	0.19	8.23	9.10	1953	1992	1951	2028	1971
Co(01-10)	148	0.64	0.16	8.68	9.47	1919	1960	1917	1996	1938
Co(10-12)	169	0.66	0.16	8.69	9.51	1915	1956	1913	1993	1934
Edge	110	0.64	0.10	9.30	10.03	1867	1910	1864	1948	1886
Corner (a)	125	0.69	0.11	8.80	9.60	1907	1948	1905	1985	1926
Corner (b)	125	0.55	0.05	9.77	10.37	1835	1879	1831	1918	1853

* There are two possible versions of this plane. This one is the parallell to the fcc (110).

unaffected (32). Beyond that, we observe that the presence of Re leads to an increase in the 2230 cm^{-1} band, in accordance with XPS (X-ray photoelectron spectroscopy) results showing a corresponding increase in the number of exposed Al atoms (1, 45).

In addition to the above effects of Re promoting, TPSR (temperature-programmed surface reaction) indicates that the presence of Re inhibits one of two reaction paths that are possible on the monometallic catalyst. The first of these two involves CO dissociation on (large) metal crystallites followed by hydrogenation of the α-carbon. The other involves spillover of CO and H to the support where a CH_xO complex is formed, followed by diffusion of the complex to (large or small) metal crystallites where it decomposes (46, 47). When Re is present, the latter path is inhibited (46) simultaneously as the number of exposed Al atoms increases. Since the formate absorption at 2908 cm^{-1} (48) is visible in both the mono- and the bimetallic catalysts, we suggest that Re either by direct blocking or by sterical hindrance inhibits the transportation of formate onto the active Co sites. If this transportation is based on migration along the catalyst surface, Re might for instance be situated near the interface between the metal and the support.

It is also of interest to know how close the contact must be between the Co and Re atoms in order to obtain the promoting effects. We know that cobalt has a close-packed hexagonal structure (ε-Co) at ordinary temperatures, but transforms to a face-centered cubic structure (α-Co) at approximately 417°C (49, p. 170). Accordingly, the presence of rhenium allows a better reduction of cobalt below this transformation temperature. A close contact between the two metals might also increase the actual transformation temperature, as a 1% alloying addition of Re to ε-Co has been reported to lead to a rise in the transition temperature of 63°C (49, p. 197). It has been suggested that rhenium promotes the reduction of cobalt oxide by hydrogen spillover (34, 35), and that no direct contact is necessary in order to obtain the promoting effects (34). The band structures arising from CO adsorbed on respectively Co and Re in the bimetallic catalyst show no shift in wavenumbers compared to the corresponding monometallic samples. This indicates that there are no strong electronic effects between the two metals, in agreement with the spillover theory.

The general increase that we observed in the intensity maximum and in the corresponding wavenumber as a function of time or increasing temperature (Figs. 3a–3e), we connect with the increasing surface coverage of CO. An increase in the coverage of CO will often appear as a blue shift in the intensity maximum. This is due to the "long-range dipole–dipole interaction," which can influence vibrations that are close in wavenumbers (1, 43, 44). The fall in intensity as a function of time and high temperatures (Figs. 3f–3i, 4), we ascribe to an increase in the amount of dissociated CO on the metal surface and a subsequent decrease in the dipole–dipole interaction (1). With regard to the absorption at 2030 cm^{-1} (Figs. 3a, 3b), both Co and Re carbonyls show distinct bands at this wavenumber (1, 42). However, the intensity increase that follows the temperature raise from room temperature to 100°C does not really fit with the corresponding spectra of the Re catalyst (50). The intensity increase is therefore ascribed to an increase in the amount of Co carbonyl species on the catalyst surface.

Absorbances due to CO adsorbed on Re atoms are observed at 2035, 1925, and 1895(sh) cm^{-1} when the catalyst after CO adsorption is exposed to oxygen or hydrogen (Figs. 5 and 6). This triplet is previously ascribed to tricarbonyl species adsorbed on Re (42); see also Table 2.

Other absorption maxima are observed between the two bands at 2035 and 1929 cm^{-1} during the hydrogenation process (Fig. 7). Moreover, very low CO pressures at 200°C reveal various intensity maxima that at higher pressures are concealed by other more intense absorptions (Fig. 8). In this latter case, we observe either (i) a single absorption band at 1920–29 cm^{-1}, or (ii) various combinations the

TABLE 2

Assignment of Absorptions Appearing in the Spectrum of CO Adsorbed on 1% Re/γ-Al_2O_3 (50)

Species	Wavenumbers/cm^{-1}
ReCO	2030
$Re(CO)_3$	2035, 1925, 1895
$Re(CO)_4$	2107, 2040, 1990

following bands: 1970–95, 1938–50, 1900–1897, 1806–20, and 1791–1800 cm^{-1}.

In one case, vibrational bands at 2057, 2033, 1990(sh), 1937, 1937–45, 1893, and 1867 cm^{-1} also developed after Fischer–Tropsch activity followed by exposure to CO(g) for 2 days at room temperature and subsequent evacuation (Fig. 9). CO adsorbed on Co_3O_4 at room temperature has been reported to give rise to absorptions at 2070, 2060, 1980, 1950, 1905, 1880, 1822, and 1788 cm^{-1} (26). Also, a 5% Co/Al_2O_3 catalyst that was exposed to CO(g) for more than 20 h developed maxima at 2060, 2025, 1990, 1950, 1900, and 1790 cm^{-1} (2), and we have previously assigned the band around 2060 cm^{-1} to overlapping contributions from $Co(CO)_n$, CoHCO, $Co^{\delta+}$–CO, and large islands of CO^0–CO on Co(0001) (1). In the same work, the intensity maximum around 2030 cm^{-1} was ascribed to Co^0CO and $Co(CO)_n$ (1). That the band structures above reappear after re-reduction at 500°C (Fig. 9b) indicates that the structures are due to CO adsorbed on a rather well-reduced part of the Co particles. This is not necessarily in contrast to the spectral resemblance with CO adsorbed on Co_3O_4, as Co_3O_4 is easily reduced by CO even at room temperature (26).

The bands from 1990 cm^{-1} and below have previously been assigned to polycarbonyl species (2). The absorptions around 1990 and 1950 cm^{-1} are favored by CO(g) exposure time, by high temperature, and by high pressure in accordance with this interpretation. Also, the result of our theoretical calculations (1) supports the assignment of the pair of bands to $Co(CO)_n$ (Table 1). Nevertheless, it is not evident whether the 1990 and the 1950 cm^{-1} bands arise from the same species or not. The band pair shows very similar behavior to changes in the experimental conditions and fits well with the calculated wavenumbers for band pairs arising from various di- and tricarbonyls (Table 1). Assuming that the absorption bands are due to CO adsorbed on ideal surfaces, "the metal surface selection rule" is valid, and the two absorptions must arise from different species. On the other hand, "the metal surface selection rule" needs not be (strictly) valid for reconstructed surfaces. There are two reasons for this. First, species situated at defects may have a non-normal orientation with respect to the general surface. Second, surface reconstruction might affect the conductivity of the metal. In conclusion, we can neither exclude nor confirm that the 1990 and the 1950 cm^{-1} bands arise from the same carbonyl species.

The singlet around 1925 cm^{-1}, appearing when small amounts of CO(g) are introduced at 200°C (case (i), above), we assign mainly to CO adsorbed on defects, edges, or corners in accordance with Table 1. The absorptions below 1900 cm^{-1} we have earlier assigned to CO adsorbed in a polycoordinated position on well-reduced parts of the catalyst. From this interpretation, the amount of bridged species should increase with time at room temperature. This is a likely development since bridged species do not form on too small islands of reduced Co atoms, CO(g) may function as a reducing agent (26), and the CO dissociation activity is close to zero at room temperature.

Generally, we suggest that large structures of adsorbed CO are broken up during the Fischer–Tropsh activity. This may follow from carbidization, but also from a more general reconstruction of the surface that includes creation of defects, see Refs. (1, 51). First, the reconstruction leads to a decrease in the long-range dipole–dipole interaction and thereby in the intensity transfer toward higher wavenumbers. This may reveal new absorptions, which also may appear with a substantial increase in intensity (43, 44). Second, the concentration of defects increases and thereby so does the concentration of subcarbonyls. Third, a certain degree of migration might take place, and thereby lead to the formation of larger particles, which may possess properties different from those of the smaller ones. In addition, the maxima arising from prolonged contact with CO(g) at room temperature, but before the catalyst has become stabilized,[3] indicate that CO(g) may both reduce and reconstruct the cobalt surface even at low temperatures, although the process here is slower. The spectral resemblance with CO adsorbed on (at least partly reduced) Co_3O_4 might indicate that these bands are caused by CO adsorbed on Co atoms that are part of the larger Co particles. (Due to the metal–support interaction, it is natural to assume that the largest particles are formed from the reduction of well-defined Co_3O_4 crystals.)

Consistent with this picture, our spectral results indicate that the CO adsorption is close to reversible at lower temperatures (in agreement with Ref. (52)) but not at higher temperatures. The absorption bands appearing after a second introduction of CO(g) at 200°C were lower in both intensity and wavenumbers compared to the original bands. Presumptively, the evacuation process leads to a less dense adsorption pattern that facilitates the C–O dissociation and, if hydrogen is present, the possible formation of hydrocarbons. Therefore, when CO(g) is reintroduced, the readsorption is inhibited due to formation of new species and surface reconstruction. Likewise, the CO adsorption 200°C was not reproduced after a short elevation of the

---

[3] The stabilization period for Co catalysts is supposed to be at least 100 h at high pressure, probably somewhat shorter at our pressures.

temperature to 250°C. The mechanism here is probably the same, as the higher temperature may lead to increased CO dissociation and surface restructuring, which again may result in adsorbed species that remain and thereby inhibit CO adsorption when the temperature is lowered.

VI. CONCLUSIONS

The presence of Re as a promoter is shown to increase the degree of cobalt reduction, increase the amount of bridged species, and decrease the reduction temperature. The absorption bands due to Re carbonyls confirm the existence of Re at the catalyst surface simultaneously as there seems to be no electronic effect between the promoter and the active metal. These observations support the theory that the improved reduction of cobalt oxide in this catalyst is due to hydrogen spillover from rhenium.

Re is known to block the reaction path involving both the support and the metal. The formation of formate on the support seems to be unchanged by the presence of the promoter. We suggest that Re either by direct blocking or by sterical hindrance inhibits the transportation of formate from the support to the metal.

We observe that prolonged exposure to CO may lead to a reconstruction of the Co surface. This process involves creation/destruction of various adsorption sites and leads to a decrease in the long-range dipole–dipole interaction. Accordingly, new absorptions are revealed in the spectrum.

ACKNOWLEDGMENTS

The authors gratefully acknowledge the Norwegian Research Council and Statoil for financial support. We also acknowledge the Norwegian Institute of Technology for supplying catalyst samples. We thank Professor II Ole Henrik Ellestad and Professor Peter Klæboe for their helpful discussions.

REFERENCES

1. Rygh, L. E. S., Ellestad, O. H., Klaeboe, P., and Nielsen, C. J., *Phys. Chem. Chem. Phys.* **2**, 1835 (2000).
2. Kadinov, G., Bonev, Ch., and Palazov, A., *J. Chem. Soc., Faraday Trans.* **94**, 3027 (1998).
3. Todorova, S., Zhelyazkov, V., Zhelyakov, V., and Kadinov, G., *React. Kinet. Catal. Lett.* **57**, 105 (1996).
4. Fredriksen, G. R., Blekkan, E. A., Schancke, D., and Holmen, A., *Chem. Eng. Technol.* **18**, 125 (1995).
5. Fredriksen, G. R., Blekkan, E. A., Schancke, D., and Holmen, A., *Ber. Bunsenges. Phys. Chem.* **97**, 308 (1993).
6. Lapidus, A., Krylova, A., Kazanskii, V., Borokov, V., and Zaitsev, A., *Appl. Catal.* **73**, 65 (1991).
7. Kazanskii, V. B., Zaitsev, A. V., Borokov, V. Yu., and Lapidus, A. L., *Appl. Catal.* **40**, 17 (1988).
8. Zaitsev, A. V., Krasnova, L. L., Savel'ev, M. M., Borokov, V. Yu., Lapidus, A. L., and Kazanskii, V. B., *Kinet. Catal.* **28**, 1194 (1987).
9. Kuznetsov, V. L., Aleksandrov, M. N., and Bulgakova, L. N., *J. Mol. Catal.* **55**, 146 (1989).
10. Choi, J.-G., Rhee, H.-K., and Moon, S. H., *Appl. Catal.* **13**, 269 (1985).
11. Choi, J.-G., Rhee, H.-K., and Moon, S. H., *Kor. J. Chem. Eng.* **1**, 159 (1984).
12. Lahtinen, J., Anraku, T., and Somorjai, G. A., *Catal. Lett.* **25**, 241 (1994).
13. Cabrera, A. L., Garrido, W. H., and Volkmann, U. G., *Catal. Lett.* **25**, 115 (1994).
14. Lahtinen, J., Anraku, T., and Somorjai, G. A., *J. Catal.* **142**, 206 (1993).
15. Kuhn, W. K., He, J.-W., and Goodman, D. W., *in* "Surface Science of Catalysis" ACS Symp. Ser. Surf. Sci. Catal., pp. 71–84. Am. Chem. Soc., Washington, DC, 1992.
16. He, J.-W., Kuhn, W. K., and Goodman, D. W., *J. Am. Chem. Soc.* **113**, 6416 (1992).
17. Wojtzac, J., Queau, R., and Poilblanc, R., *J. Catal.* **37**, 391 (1975).
18. Queau, R., and Poilblanc, R., *J. Catal.* **27**, 200 (1972).
19. Blyholder, G., and Allen, M. C., *J. Am. Chem. Soc.* **91**, 3158 (1969).
20. Baker, F. S., Bradshaw, A. M., Pritchard, J., and Sykes, K. W., *Surf. Sci.* **12**, 426 (1968).
21. Kavtaradze, N. N., and Sokolova, N. P., *Russ. J. Phys. Chem.* **38**, 548 (1964).
22. Beitel, G. A., deGroot, C. P. M., Oosterbeek, H., and Wilson, J. H., *J. Phys. Chem.* **101**, 4035 (1997).
23. Beitel, G. A., Laskov, A., Oosterbeek, H., and Kuipers, E. W., *J. Phys. Chem.* **100**, 12494 (1996).
24. Toomes, R. L., and King, D. A., *Surf. Sci.* **349**, 1 (1996).
25. Geerlings, J. J. C., Zonnevylle, M. C., and De Groot, C. P. M., *Catal. Lett.* **5**, 309 (1990).
26. Busca, G., Guidetti, R., and Lorenzelli, V., *J. Chem. Soc., Faraday Trans.* **86**, 989 (1990).
27. Sweany, R. L., and Brown, T. L., *Inorg. Chem.* **16**, 415 (1997).
28. Sweany, R. L., and Brown, T. L., *Inorg. Chem.* **16**, 421 (1997).
29. Brienne, S. H., Markwell, R. D., Barnett, S. M., Butler, I. S., and Finch, J. A., *Appl. Spectrosc.* **47**, 1131 (1993).
30. Hanlan, L. A., Huber, H., Kündig, E. P., McGarvey, B. R., and Ozin, G. A., *J. Am. Chem. Soc.* **26**, 7054 (1975).
31. Busca, G., Lorenzelli, V., Escribano, V. S., and Guidetti, R., *J. Catal.* **131**, 167 (1991).
32. Vada, S., Hoff, A., Ådnanes, E., Schanke, D., and Holmen, A., *Topics Catal.* **2**, 155 (1995).
33. Hoff, A., Ph.D. Eng. Thesis, Norwegian Institute of Technology, October 1993.
34. Hilmen, A. M., Schancke, D., and Holmen, A., *Catal. Lett.* **38**, 143 (1996).
35. Matsuaki, T., Takeuchi, K., Hanaoka, T., Arakawa, H., and Sugi, Y., *Catal. Today* **28**, 251 (1996).
36. Every, K. W. V., and Griffiths, P. R., *Appl. Spectrosc.* **45**, 347 (1991).
37. Hamadeh, I. M., and Griffiths, P. R., *Appl. Spectrosc.* **41**, 682 (1987).
38. Timney, J. A., *Inorg. Chem.* **18**, 2502 (1979).
39. Anderson, A. B., *in* "Theoretical Aspects of Heterogeneous Catalysis" (J. B. Moffat, Ed.), pp. 431–457. Van Nostrand, New York, 1990.
40. Calzaferri, G., Forss, L., and Kamber, I., *J. Phys. Chem.* **93**, 5366 (1989).
41. Calzaferri, G., and Brändle, M., Quantum chemistry program performing extended Hückel calculations, Quantum Chemistry Program Exchange, QCPE No. QCMP 116, 1992.
42. Rygh, L. E. S., Gausemel, I., Ellestad, O. H., Klaeboe, P., Nielsen, C. J., and Rytter, E., *J. Mol. Struct.* **349**, 325 (1995).
43. Ryberg, R., *Adv. Chem. Phys.* 1–43 (1989).
44. Persson, B. N. J., and Ryberg, R., *Phys. Rev. B* **24**, 6954 (1981).
45. Rytter, E., Statoil Research Center, Trondheim, personal communication.
46. Araya, A.-K., Aas, N., and Rytter, E., Poster, Europacat-II, Maastricht 1995.
47. Lee, W. H., and Bartolomew, C. H., *J. Catal.* **120**, 256 (1989).
48. Tamaru, K., and Onishi, T., *Appl. Spectrosc. Rev.* **9**, 133 (1975).
49. Centre d'Information du Cobalt C.I.C Ed., Cobalt Monograph, C.I.C., Brussel, 1960.
50. Gausemel, I, M.Sc. Thesis, University of Oslo, June 1994.
51. Wilson, J., and de Groot, C., *J. Phys. Chem.* **99**, 7860 (1995).
52. Reuel, R. C., and Bartholomew, C. H., *J. Catal.* **85**, 63 (1984).